

Topological order and thermal equilibrium in polariton condensates

Davide Caputo,^{1,2} Dario Ballarini,¹ Galbadrakh Dagvadorj,^{3,4} Carlos Sánchez Muñoz,⁵
Milena De Giorgi,¹ Lorenzo Dominici,¹ Kenneth West,⁶ Loren N. Pfeiffer,⁶
Giuseppe Gigli,^{1,2} Fabrice P. Laussy,^{7,8} Marzena H. Szymańska,³ and Daniele Sanvitto^{1,9}

¹*CNR NANOTEC—Institute of Nanotechnology, Via Monteroni, 73100 Lecce, Italy*

²*University of Salento, Via Arnesano, 73100 Lecce, Italy*

³*Department of Physics and Astronomy, University College London,
Gower Street, London WC1E 6BT, United Kingdom*

⁴*Department of Physics, University of Warwick, Coventry CV4 7AL, United Kingdom*

⁵*CEMS, RIKEN, Saitama, 351-0198, Japan*

⁶*PRISM, Princeton Institute for the Science and Technology of Materials,
Princeton University, Princeton, NJ 08540*

⁷*Faculty of Science and Engineering, University of Wolverhampton,
Wulfruna St, WV1 1LY, United Kingdom*

⁸*Russian Quantum Center, Novaya 100, 143025 Skolkovo, Moscow Region, Russia*

⁹*INFN, Sez. Lecce, 73100 Lecce, Italy*

We report the observation of the Berezinskii-Kosterlitz-Thouless transition for a 2D gas of exciton-polaritons – bosonic light-matter particles – in semiconductor microcavities. Differently from the case of ultracold atoms, the joint measurement of the first-order coherence both in space and time is required to characterize the phase transition in this driven-dissipative system. The observed quasi-ordered phase, characteristic for an equilibrium 2D bosonic gas, with a decay of coherence in both spatial and temporal domains with the same algebraic exponent, is reproduced with numerical solutions of stochastic dynamics, proving that the mechanism of pairing of the topological defects (vortices) is responsible for the transition to the algebraic order. This is made possible thanks to long polariton lifetimes in high-quality samples with small disorder and in a reservoir-free region far away from the excitation spot. These results open the way to the investigation of topological ordering in open systems and of out-of-equilibrium phase transitions in optical microcavities.

Collective phenomena which involve the emergence of an ordered phase in many-body systems have a tremendous relevance in almost all fields of knowledge, spanning from physics to biology and social dynamics^{1,2}. While the physical mechanisms can be very different depending on the sys-

tem considered, statistical mechanics aims at providing universal descriptions of phase transitions on the basis of few and general parameters, the most important ones being dimensionality and symmetry³⁻⁵. The spontaneous symmetry breaking of Bose–Einstein condensates (BEC) below a critical temperature $T_C > 0$ is a remarkable example of such a transition, with the emergence of an extended coherence giving rise to a long range order (LRO)⁶⁻⁸. Notably, in infinite systems with dimensionality $d \leq 2$, true LRO cannot be established at any finite temperature⁹. This is fundamentally due to the presence of low-energy, long-wavelength thermal fluctuations (i.e. Goldstone modes) that prevail in $d \leq 2$ geometries.

BKT phase transition

However, if we accept a lower degree of order, characterised by an algebraic decay of coherence, it is still possible to make a clear distinction between such a quasi-long-range-ordered (QLRO) and a disordered phase in which the coherence is lost in a much faster, exponential way. Such transitions, in two dimensions (2D) and at a critical temperature $T_{\text{BKT}} > 0$, are explained in the Berezinskii–Kosterlitz–Thouless theory (BKT) by the proliferation of vortices—the fundamental topological defects—of opposite signs¹⁰. This theory is well established for 2D ensembles of cold atoms in thermodynamic equilibrium, where the transition is linked to the appearance of a linear relationship between the energy and the wavevector of the excitations in the quasi-ordered state¹¹. The joint observation of spatial and temporal decay of coherence has never been observed in atomic systems, mainly because of technical difficulties in measuring long-time correlations. These are important observables to bring together because an algebraic decay, with the same exponent α , for both the temporal and spatial correlations of the condensed state, implies a linear dispersion for the elementary excitations¹²⁻¹⁴.

Phase transition in open systems

On the other hand, semiconductor systems such as microcavity polaritons (dressed photons with sizeable interactions mediated by the excitonic component) appear to be, since the report of their condensation¹⁵⁻¹⁷, ideal platforms to extend the investigation of many-body physics to the more general scenario of phase transitions in driven-dissipative systems¹⁸. However, establishing if the transition can actually be governed by the same BKT process as for equilibrium system has proven to be challenging from both the theoretical¹⁹⁻²¹ and experimental perspective²²⁻²⁴. Indeed, the dynamics of phase fluctuations is strongly modified by pumping and dissipation, and the direct measurement of their dispersion by photoluminescence and four-wave-mixing experiments is limited by the short polariton lifetime, by the pumping-induced noise and by the low resolution close to

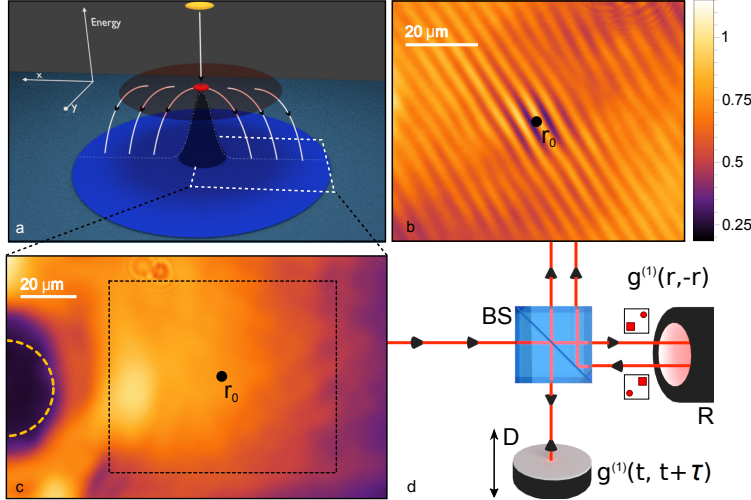


Figure 1. **Pumping mechanism and interferometric setup.** **a**, Sketch of polariton relaxation in space (x, y) and energy (vertical axis). The carriers, injected by the pumping laser, relax quickly into excitonic states (yellow area) spatially confined within the pumping spot region. Efficient scattering from the exciton reservoir into polariton states results in a region of high polariton density (red area) which expands radially. During the expansion, the long lifetime allows for polariton relaxation into lower energy states and eventually, at high power, into the ground state. Above a threshold power, an extended 2D polariton condensate (blue area) is formed outside of the pumped region. **b**, Interferogram of the region in the black-dashed rectangle in **c**. The black dot at the centre indicates the autocorrelation point r_0 . **c**, 2D real-space image of the emitted light (arbitrary intensity units in color scale) from a portion of the condensate. To visualise only the bottom energy state in 2D images, the emission coming from $|k| < 1 \mu\text{m}^{-1}$ has been selected in the far field to avoid the contribution of higher energy polaritons. The yellow, dashed circle indicates the blue-shifted region corresponding to the position of the laser spot. **d**, Scheme of the interferometric setup: R=retroreflector, BS=beam splitter, D=long delay line. The retroreflector R is a 3-mirror corner reflector used to reflect the image at the central point r_0 before sending it back towards the BS.

66 the energy of the condensate. Moreover, the algebraic decay of coherence has been experimentally
 67 demonstrated only in spatial correlations, while only exponential or Gaussian decays of temporal
 68 coherence, which are not compatible with a BKT transition, have been reported until now²⁵⁻²⁸.
 69 The lack of a power-law decay of temporal correlations is a robust argument against a true BKT
 70 transition, as will be demonstrated later on with a straightforward counter-example of a strongly
 71 out-of-equilibrium system. For this reason, it has been a constant matter of interest what is the
 72 nature of the various polariton phases, what are the observables that allow to determine a QLRO,
 73 if any, and how they compare with equilibrium 2D condensates and with lasers²⁹⁻³⁵.

Equilibrium vs out-of-equilibrium

74
 75 Recently, thanks to a new generation of samples with record polariton lifetimes, the thermaliza-
 76 tion across the condensation threshold has been reported via constrained fitting to Bose–Einstein
 77 distribution, suggesting a weaker effect of dissipation in these systems³⁶. However, to unravel the
 78 mechanisms that drive the transition, and characterize its departure from the equilibrium condition,
 79 it is crucial to measure the correlations between distant points in space and time as we move from
 80 the disordered to the quasi-ordered regime^{13,14,37,38}. So far, all attempts in this direction have been
 81 thwarted, not only because of the polariton lifetime being much shorter than the thermalization
 82 time and the fragmentation induced by sample inhomogeneities^{39,40}, but also because of the small
 83 extents of the condensate. Indeed, earlier measurements of coherence^{25,41,42} were limited to the
 84 small spatial extension of the exciton reservoir set by the excitation spot, which could result in an
 85 effective trapping mechanism⁴³ and finite-size effects³⁰.

BKT transition in exciton-polaritons

86
 87 In this work, using a high quality sample (in terms of long lifetimes and spatial homogeneity) to form
 88 and control a reservoir-free condensate of polaritons over a largely extended spatial region, we make
 89 the first observation in any system of the transition to a QLRO phase both in spatial and in temporal
 90 domains. Remarkably, the convergence of spatial and temporal decay of coherence allows us to
 91 identify the connection with the classic equilibrium BKT scenario, in which for systems with linear
 92 spectrum the exponents take exactly the same value $\alpha \leq 1/4$ ¹⁴. Stochastic simulations tuned to
 93 the experimental conditions, that reproduce the experimental observations in both space and time,
 94 further allow us to track vortices in each realisation of the condensate, confirming the topological
 95 origin of the transition. All these results settle the BKT nature of the 2D phase-transition for
 96 polaritons in high quality samples, providing the equilibrium limit of driven/dissipative systems.
 97 For shorter lifetimes, it is known that the transition departs from the equilibrium condition²⁸ and,
 98 at larger densities, different mechanisms will prevail over topological ordering⁴⁴. We show here that
 99 for a strongly out-of-equilibrium microcavity (in the weak coupling regime), the power-law decay of
 100 the first order coherence is observed only in space but not in time. We therefore demonstrate not
 101 only that low-density polariton condensates can undergo an equilibrium BKT transition like cold
 102 atoms, but also that spatial correlations alone do not allow to distinguish between a photon laser
 103 and a BKT phase.

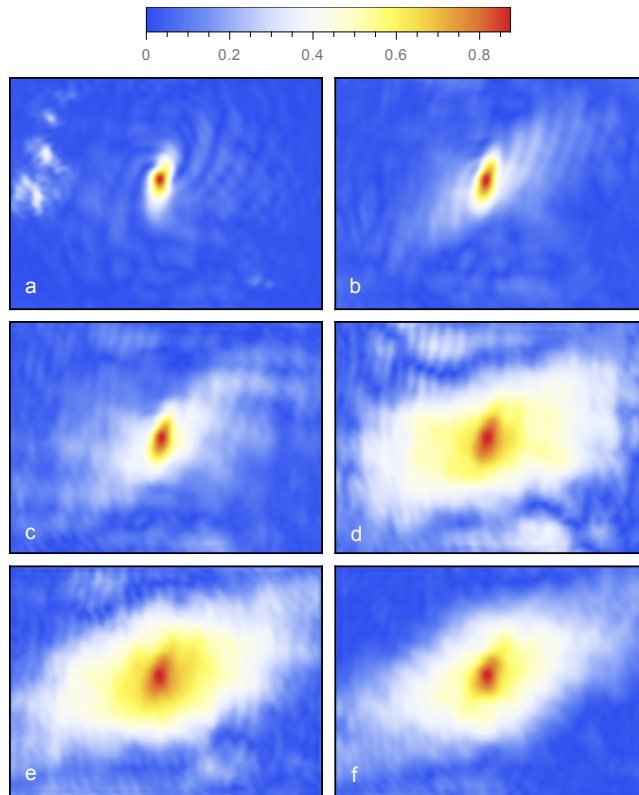


Figure 2. **Two dimensional first order spatial correlations.** Maps of $|g^{(1)}(\mathbf{r})|$ as extracted from the interferogram (Fig. 1b) relative to an area of the sample of about $80\ \mu\text{m} \times 60\ \mu\text{m}$ and corresponding to different densities $d = (0.05, 0.3, 0.5, 1.3, 3, 4)d_{\text{th}}$ in (a, b, c, d, e, f) respectively.

104

Formation of a polariton condensate

105 The mechanism used to form an extended polariton condensate is sketched in Fig. 1a. The sample
 106 is excited non-resonantly (details in Supplementary Information), leading to the formation of an
 107 exciton reservoir (yellow region in Fig. 1a) which is localised within the pumping spot area due to
 108 the low exciton mobility. In turn, the repulsive interactions between excitons induce a blueshift
 109 of the polariton energy at the centre of the pumping spot (the dashed-white line in Fig. 1a shows
 110 the contour along the x direction and crossing the excitation spot). As can be seen, the exciting
 111 beam generates an energy blueshift corresponding to the Gaussian profile of the laser. Polaritons,
 112 which are formed in the exciton reservoir through energy relaxation, are much lighter particles than
 113 excitons and are accelerated outwards from the centre of the spot by the potential landscape^{45,46}.
 114 We have recently demonstrated that in high quality 2D samples, the cloud of expanding polaritons
 115 relaxes through incoherent scattering processes into the ground state: when the stimulated scatter-
 116 ing prevails over losses, a uniform polariton condensate is formed over a wide spatial region outside

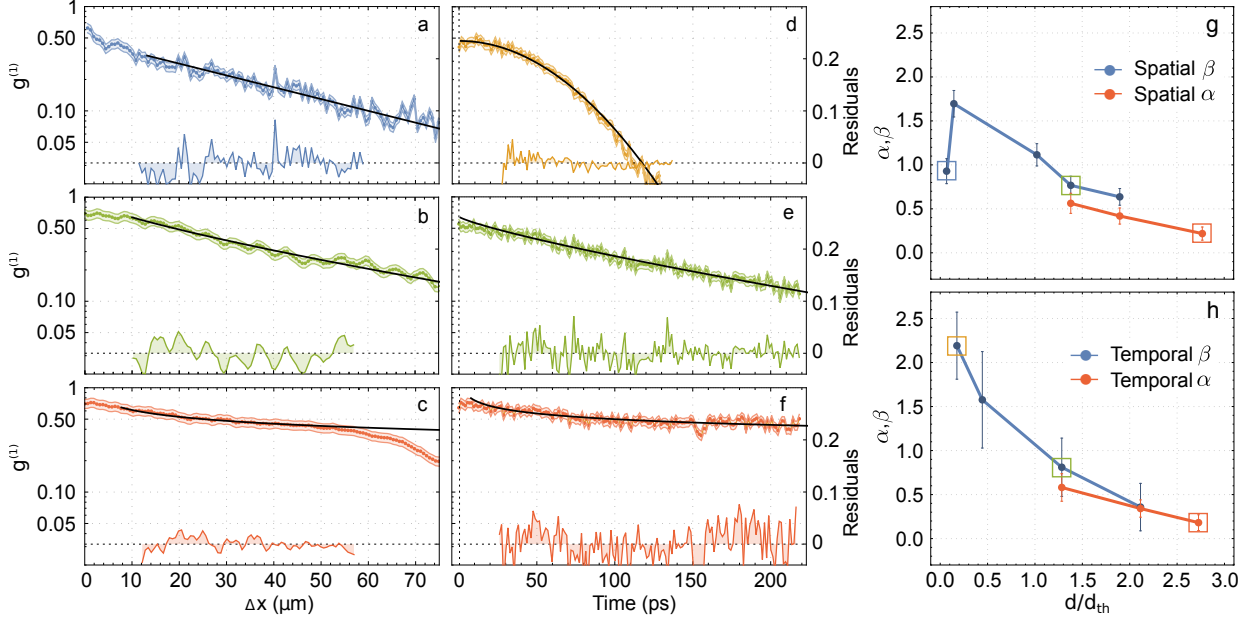


Figure 3. **Coherence decay and BKT phase transition.** **a, b, c**, Spatial decay of $|g^{(1)}(\Delta x)|$ (logarithmic scale) and corresponding fitting residuals (linear scale) for: **a**, $d = 0.1d_{th}$ exponential decay (blue data), **b**, $d = 1.4d_{th}$ stretched exponential decay (green data), **c**, $d = 2.75d_{th}$ power-law decay (red data). **d, e, f**, Temporal decay of $|g^{(1)}(\Delta t)|$ (logarithmic scale) and corresponding fitting residuals (linear scale) for: **d**, $d = 0.15d_{th}$ Gaussian decay (yellow data), **e**, $d = 1.3d_{th}$ stretched exponential decay (green data), **f**, $d = 2.7d_{th}$ power-law decay (red data). Note that the value of $|g^{(1)}(0)| < 1$ is due to the time-averaged detection that globally reduces the visibility of the interferograms, without changing the slope of the correlations decay (see Supplementary Information). **g, h**, Blue line: β exponent evaluated by stretched-exponential fitting of $|g^{(1)}(\Delta x)|$ in **g**, and $|g^{(1)}(\Delta t)|$ in **h**, versus the corresponding polariton densities. Red line: α exponent evaluated by power-law fitting of $|g^{(1)}(\Delta x)|$ in **g**, and $|g^{(1)}(\Delta t)|$ in **h**, versus the corresponding polariton densities. The same color legend used in panels **a, b, c** and **d, e, f** indicates the corresponding densities (square markers) in panels **g** and **h**. Error bars are obtained from the fitting parameters (see Supplementary Information).

117 the area of the pumping spot⁴⁷. The light emitted by the sample carries all the information about
 118 the spatio-temporal correlations of the polariton field, that can be extracted as follows: the interfer-
 119 ograms (Fig. 1b) are obtained selecting a sample region without the exciton reservoir, such as the
 120 one indicated by a dashed rectangle in Fig. 1c, that is directed into the Michelson interferometer
 121 outlined in Fig. 1d. Here, the image is duplicated in the beam splitter and reflected around the
 122 central point \mathbf{r}_0 in one arm of the interferometer, giving the interferogram shown in Fig. 1b. The
 123 first order correlation function at equal time $g^{(1)}(\mathbf{r}, -\mathbf{r})$ ($\mathbf{r}_0 = 0$ is assumed) can then be measured
 124 between any two points symmetric about \mathbf{r}_0 as a function of their separation $|\mathbf{2r}|$ following the same

125 method used in Ref. [16] and reported in the Supplementary Information. The temporal coherence
 126 $g^{(1)}(t, t + \Delta t)$ is measured by moving the long delay line, covering a distance corresponding to a
 127 temporal delay of more than 200 ps.

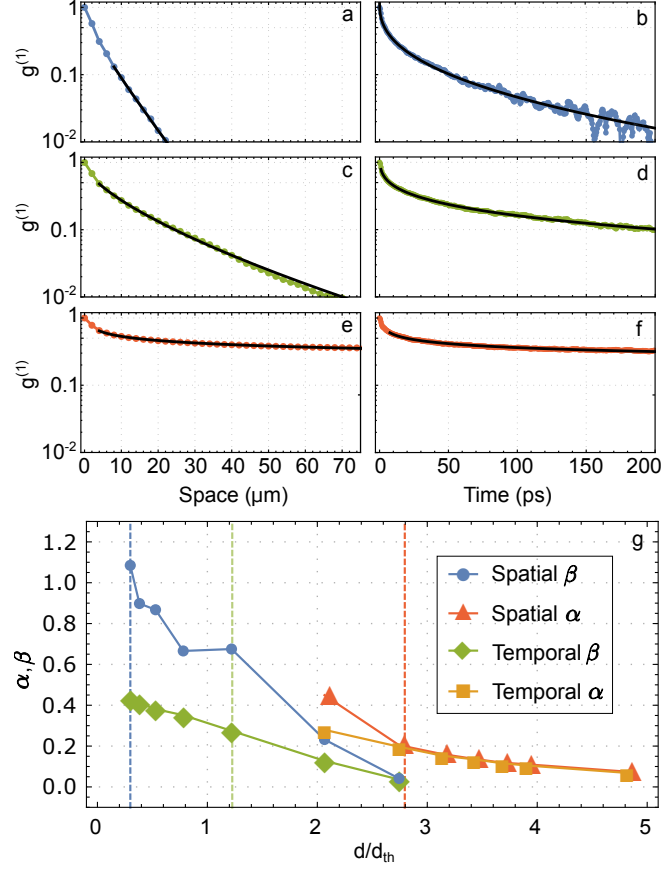


Figure 4. **Decay of coherence from stochastic analysis of a homogeneous system.** **a,c,e** Spatial decay of coherence. Respectively, an exponential decay, a stretched exponential with $\beta = 0.67$ and a power-law decay with $\alpha = 0.20$. **b,d,f**, Temporal decay of coherence. Respectively, a stretched exponential with $\beta = 0.41$, a stretched exponential with $\beta = 0.27$ and a power law with $\alpha = 0.20$. These three cases are indicated in **g** with blue, green and red vertical dashed lines. **g**, Exponents β of the stretched exponential fit, for spatial (blue) and temporal (green). Exponents α of the power law fitting for spatial (red) and temporal (orange).

128

129

131

Spatial correlations and decay exponents

132 The 2D maps of $|g^{(1)}(\mathbf{r}, -\mathbf{r})|$, extracted from the interferograms, are shown in Fig. 2 for different
 133 values of the polariton density d in the lowest-energy state. The spatial extent of coherence, limited
 134 to the autocorrelation point at low densities (Fig. 2a-c), extends over larger distances above a
 135 threshold density d_{th} (Fig. 2d), indicating that stimulated scattering starts prevailing over losses

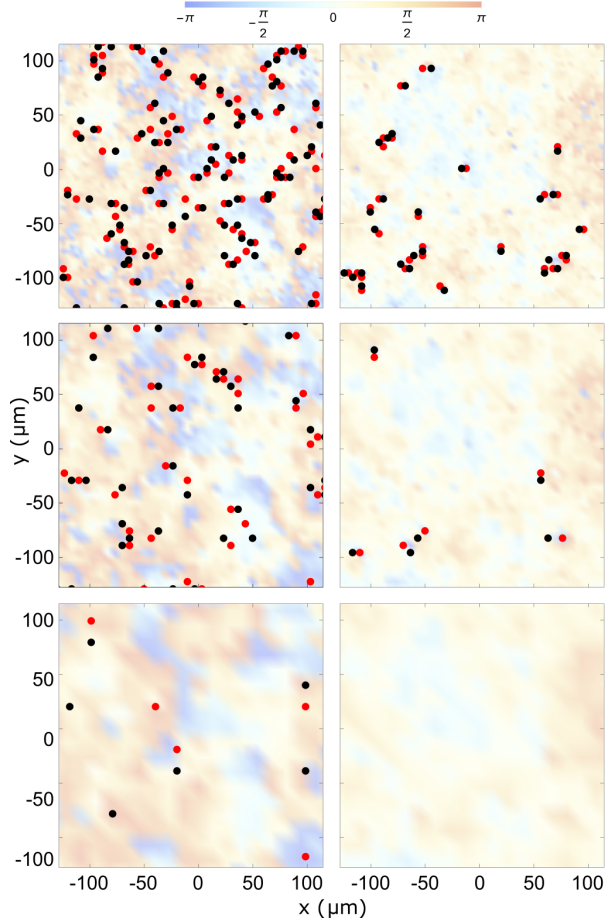


Figure 5. **Vortex-antivortex distribution map.** **Top**, Vortices (V) in red and anti-vortices (AV) in black just before (left) and after (right) the BKT transition with parameters as in Fig. 4c and e, respectively. **Middle-Bottom** The same as in **Top** but after filtering off in two steps high momentum states to eliminate bound pairs. Such filtering reveals the presence of free vortices. Note that there are no free vortices when spatial and temporal coherence show algebraic decay (right) but there are some free vortices in the case of stretched exponential decay of coherence (left). The underlying colour map shows the phase profile of the field.

136 (see Supplementary information). For larger densities, a higher level of coherence is sustained over
 137 a wider spatial region of about $80\ \mu\text{m} \times 60\ \mu\text{m}$ (Fig. 2e). The longer coherence length for $d > d_{\text{th}}$ is
 138 unrelated to the dynamics of higher energy polaritons and corresponds to the formation of a uniform
 139 phase in the ground state over distances much larger than the healing length (see Supplementary
 140 Information). As shown in Fig. 2f, increasing further the excitation power results in the shrinking
 141 of the spatial extension of coherence due to the additional dephasing induced by the pump and the
 142 formation of excited states at higher energies⁴⁶.

In Fig. 3, we analyse the behaviour of coherence close to the density threshold in a more quan-

titative way. The horizontal line profile of $|g^{(1)}(x, -x)|$ passing through \mathbf{r}_0 , for $\Delta x > 0$ (with $\Delta x \equiv 2x$), is studied for increasing pumping powers (Fig. 3(a-c)). To allow a uniform description across the transition, both power law and stretched exponential functions are used in the fitting procedure:

$$|g^{(1)}(x, -x)| = A|2x|^{-\alpha} \quad (1)$$

$$|g^{(1)}(x, -x)| = Ae^{-B|2x|^\beta}, \quad (2)$$

143 with B a scale parameter for the x -axis and $A \leq 1$ a space-independent amplitude factor (see
 144 Supplementary Information). For $d < d_{\text{th}}$, the decay is exponential and it is well fitted by eq. (2)
 145 with $\beta \approx 1$ (Fig. 3a). Approaching $d = d_{\text{th}}$, the spatial decay of $g^{(1)}$ becomes slower, but still faster
 146 than a power law (Fig. 3b). This transition regime is best described by a stretched exponential
 147 decay ($\beta < 1$) that becomes a power-law only at slightly higher densities $d \approx 2.7 d_{\text{th}}$ (Fig. 3c) when
 148 a high degree of spatial coherence ($>50\%$) extends over distances of $\approx 50 \mu\text{m}$. Remarkably, the
 149 slow decay shown in Fig. 3c can be best characterised by the exponent $\alpha = 0.22$ (see Supplementary
 150 Information for a comparison between the different functional behaviours). In Fig. 3g, the α and
 151 β exponents are reported for different densities (α can be extracted only for $d > d_{\text{th}}$), showing the
 152 whole behaviour of the coherence decay across the transition into the QLRO. However, as will be
 153 shown in the following, it is essential to verify that a similar behaviour is also observed for the
 154 temporal correlations.

155 Temporal correlations

156 In Fig. 3(d-f), the temporal coherence at the autocorrelation point $|g^{(1)}(t, t + \Delta t)|$ is shown for three
 157 different polariton densities. In Fig. 3h, the α and β exponents of equations (1) and (2) that best fit
 158 the experimental data are shown across the transition. Below threshold, coherence decays quickly
 159 and follows a Gaussian slope ($\beta \approx 2$). At $d = 1.3 d_{\text{th}}$, the temporal coherence can be best fitted by
 160 (2) with an exponent $\beta \approx 0.8$ (or, with a slightly worst fit, with a power law of exponent $\alpha \approx 0.57$),
 161 while at $d \approx 2.7 d_{\text{th}}$, the long time behaviour clearly follows a power law with $\alpha = 0.2$. The
 162 residuals analysis proves the agreement between the experimental data and the fitting model (see
 163 Supplementary Information). Crucially, also for time correlations, $\alpha < 0.25$, which coincides, within
 164 the experimental accuracy, with the one obtained from the spatial coherence at the corresponding
 165 density.

Exact simulations for an homogeneous systems

166

167 We performed complementary theoretical analysis, based on the exact solution of the stochastic
 168 equations of motions²¹, with the same microscopic parameters as the ones of the experiment. Our
 169 approach, which can be derived either from Keldysh field theory⁴⁸ or the Fokker-Planck equations
 170 for the Wigner function¹⁸, is able to treat fluctuations beyond the mean field approximations and
 171 describes the dynamics of the whole field, accounting for both normal and superfluid polaritons (see
 172 Supplementary Information). Differently from previous works²⁵, the condensate forms outside of
 173 the exciton reservoir, that is therefore not included in the model. Moreover, the process of injection
 174 and expansion of polaritons is described as an effective pumping mechanism, without assuming any
 175 particular constrain on the incoherent polariton population, and also the energy relaxation is not
 176 externally imposed by any specific term, given that the whole physics, including thermalisation
 177 and condensation, can be self-consistently obtained from the stochastic model (see Supplementary
 178 Information). This is indeed the most general setting used in statistical mechanics to describe
 179 the effect of external driving, dissipation and many-body interactions on the phase transitions in
 180 open quantum systems^{38,48}. Here we observe the same crossover from an exponential via stretched
 181 exponential to an algebraic decay of coherence in space and time (Fig. 4) as for the experimental
 182 measurements. In particular, we see the spatial and temporal α being the same and always smaller
 183 than 1/4 above the BKT threshold (Fig. 4g), showing that the drive and dissipation do not prevail
 184 in this good quality sample in contrast to the earlier studied non-equilibrium cases^{21,25}.

185 Additionally, while the vortex-antivortex binding cannot be directly observed in the experiments,
 186 which average over many realisations, the numerical analysis is able to track the presence of free
 187 vortices in each single realisation, confirming the topological origin of the transition. Indeed, we
 188 see clearly that, in the algebraically ordered state, free vortices do not survive and the pairing is
 189 complete (Fig. 5 right column). In contrast, the exponential and stretched-exponential regimes both
 190 show the presence of free vortices (Fig. 5 left), the number of which decreases as we move across the
 191 transition. Since the stretched exponential phase is always associated with some presence of free
 192 vortices, this supports that we are observing a BKT crossover rather than a Kardar-Parisi-Zhang
 193 (KPZ) phase¹⁹. It is interesting to note here that the KPZ physics is indeed the paradigmatic
 194 model for a genuinely non-equilibrium phase transition and its manifestation in the optical domain
 195 of polariton condensates is currently at the centre of intense investigation³⁸. However, the expected
 196 critical length for the KPZ phase is beyond the experimentally achievable length-scales in our long-
 197 lifetime, incoherently driven microcavity (see Supplementary Information for further discussion).

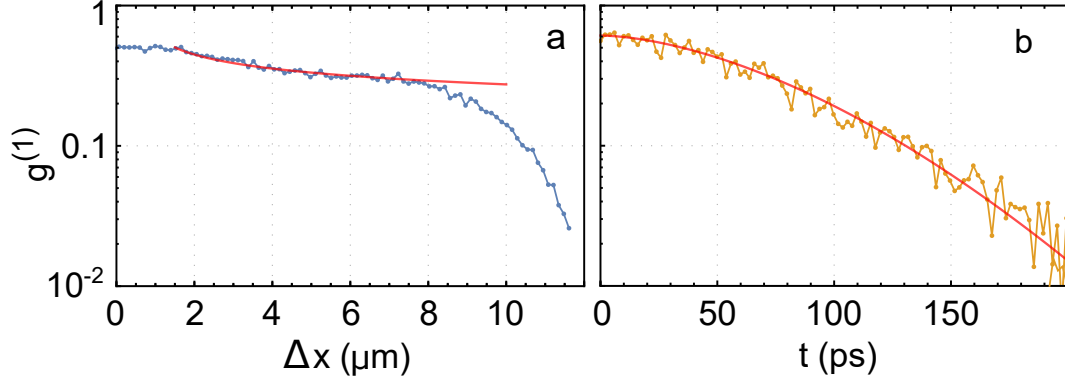


Figure 6. **Spatial and temporal coherence in weak coupling regime.** **a**, Spatial coherence showing a power-law decay with $\alpha = 0.25$. **b**, Temporal decay of coherence with stretched exponential fitting exponent $\beta = 1.8$.

198

Temporal correlations for a VCSEL

199 Finally, to demonstrate the importance of the simultaneous observation of space and time correla-
 200 tions for optical systems, and in general as we move from equilibrium towards out-of-equilibrium,
 201 we analyze the coherence behaviour of a microcavity where driven/dissipative dynamics clearly
 202 prevail. Using a sample with a lower quality factor and less quantum wells, we induce, under
 203 high non-resonant pumping, the photon-laser regime as in a vertical cavity surface emitting laser
 204 (VCSEL)^{44,49}. Despite the fact that this system is strongly out-of-equilibrium, it shows a power-law
 205 decay of spatial coherence with $\alpha = 0.25$ (Fig. 6a) within the pumping spot region (with a radius
 206 of about $10\ \mu\text{m}$). Remarkably, the behaviour of spatial correlations is very similar to what obtained
 207 in Ref [25], but the temporal coherence, shown in Fig. 6b, follows a quasi-Gaussian decay, not
 208 compatible with the algebraic order characteristic of the BKT phase. This shows that a consistent
 209 behaviour between time and space is necessary to evidence the BKT transition in driven/dissipative
 210 systems.

211

Outlook

212 The formation of an ordered phase in two-dimensional driven/dissipative ensembles of bosonic
 213 quasiparticles is observed in both spatial and temporal correlations across the transition. The
 214 collective behavior of exciton-polaritons in semiconductor microcavities lies at the interface between
 215 equilibrium and out-of-equilibrium phase transitions, and it has been often compared both to atomic
 216 condensates and to photon lasers. We show that the measurement of spatial correlations $g^{(1)}(\mathbf{r})$
 217 alone is not sufficient to establish whether an open/dissipative system is in the BKT phase. Instead,
 218 two distinct measurements, one in time and one in space domain, are needed. Satisfying this

219 requirement, we report a power-law decay of coherence with the onset of the algebraic order at the
 220 same relative density and comparable exponents for both space and time correlations. We should
 221 stress that the exceptionally long polariton lifetime in the present sample allows us to reach the
 222 BKT phase transition at low densities, and in a region without the excitonic reservoir, resulting
 223 in a lower level of dephasing. In our experiments, the absence of any trapping mechanism, be it
 224 from the exciton reservoir or potential minima, allows us to avoid the influence of finite-size effects
 225 in the temporal dynamics of the autocorrelation¹⁴. Simulations with stochastic equations match
 226 perfectly the experimental results and demonstrate that the underlying mechanism of the transition
 227 is of the BKT type, i.e., a topological ordering of free vortices into bound pairs, resulting in the
 228 coherence build up both in space and time. All these observations validate that polaritons can
 229 undergo phase-transitions following the standard BKT picture, and fulfill the expected conditions
 230 of thermal equilibrium despite their driven/dissipative nature. Now that the equilibrium character
 231 of polaritons becomes a tuneable parameter, the study of driven/dissipative phase transitions and
 232 of the universal scaling laws is within reach in this solid state device.

References

- 233
- 234 ¹ H. E. Stanley, Scaling, universality, and renormalization: Three pillars of modern critical phenomena.
 235 *Rev. Mod. Phys.* **71**, S358 (1999).
- 236 ² C. Castellano, S. Fortunato, V. Loreto, Statistical physics of social dynamics. *Rev. Mod. Phys.* **81**, 591
 237 (2009).
- 238 ³ L. Onsager, Crystal statistics. I. A two-dimensional model with an order-disorder transition. *Phys. Rev.*
 239 **65**, 117 (1944).
- 240 ⁴ L. D. Landau, E. M. Lifshitz. *Statistical Physics: Volume 5 (Course of Theoretical Physics)* (Butterworth-
 241 Heinemann, 1980).
- 242 ⁵ P. Hohenberg, B. Halperin, Theory of dynamic critical phenomena. *Rev. Mod. Phys.* **49**, 435 (1977).
- 243 ⁶ L. Pitaevskii, S. Stringari. *Bose–Einstein Condensation and Superfluidity* (Oxford University Press,
 244 2016).
- 245 ⁷ M. Kohl, T. Donner, S. Ritter, T. Bourdel, A. Ottl, F. Brennecke, T. Esslinger, Criticality and correlations
 246 in cold atomic gases. *Advances in Solid State Physics* **47**, 79 (2008).
- 247 ⁸ S. Braun, M. Friesdorf, M. Hodgman, S.S. Schreiber, P. Ronzheimer, A. Riera, M. Del Rey, I. Bloch, J.
 248 Eisert, U. Schneider, Emergence of coherence and the dynamics of quantum phase transitions. *PNAS*
 249 **112**, 3641 (2015).

- 250 ⁹ N. D. Mermin, H. Wagner, Absence of ferromagnetism or antiferromagnetism in one- or two-dimensional
251 isotropic heisenberg models. *Phys. Rev. Lett.* **17**, 1133 (1966).
- 252 ¹⁰ P. Minnhagen, The two-dimensional coulomb gas, vortex unbinding, and superfluid-superconducting
253 films. *Rev. Mod. Phys.* **59**, 1001–1066 (1987).
- 254 ¹¹ J. Steinhauer, R. Ozeri, N. Katz, N. Davidson, Excitation spectrum of a Bose–Einstein condensate. *Phys.*
255 *Rev. Lett.* **88**, 120407 (2002).
- 256 ¹² D. R. Nelson, J. M. Kosterlitz, Universal jump in the superfluid density of two-dimensional superfluids.
257 *Phys. Rev. Lett.* **39**, 1201–1205 (1977).
- 258 ¹³ M. H. Szymanska, J. Keeling, P. B. Littlewood, Nonequilibrium quantum condensation in an incoherently
259 pumped dissipative system. *Phys. Rev. Lett.* **96**, 230602 (2006).
- 260 ¹⁴ M. H. Szymańska, J. Keeling, P. B. Littlewood, Mean-field theory and fluctuation spectrum of a pumped
261 decaying Bose–Fermi system across the quantum condensation transition. *Phys. Rev. B* **75**, 195331
262 (2007).
- 263 ¹⁵ M. Richard, J. Kasprzak, R. Romestain, R. Andre, L. S. Dang, Spontaneous coherent phase transition
264 of polaritons in CdTe microcavities. *Phys. Rev. Lett.* **94**, 187401 (2005).
- 265 ¹⁶ J. Kasprzak, M. Richard, S. Kundermann, A. Baas, P. Jeambrun, J. M. J. Keeling, F. M. Marchetti, M. H.
266 Szymańska, R. André, J. L. Staehli, V. Savona, B. Littlewood, B. Deveaud, Le Si Dang, Bose–Einstein
267 condensation of exciton polaritons. *Nature* **443**, 409 (2006).
- 268 ¹⁷ R. Balili, V. Hartwell, D. Snoke, L. Pfeiffer, K. West, Bose–Einstein Condensation of Microcavity Po-
269 laritons in a Trap. *Science* **316**, 1007 (2007).
- 270 ¹⁸ I. Carusotto, C. Ciuti, Quantum fluids of light. *Rev. Mod. Phys.* **85**, 299 (2013).
- 271 ¹⁹ E. Altman, L. M. Sieberer, L. Chen, S. Diehl, J. Toner, Two-dimensional superfluidity of exciton polari-
272 tons requires strong anisotropy. *Phys. Rev. X* **5**, 011017 (2015).
- 273 ²⁰ G. Wachtel, L. Sieberer, S. Diehl, E. Altman, Electrodynamical duality and vortex unbinding in driven-
274 dissipative condensates. arXiv:1604.01042v2 (2016).
- 275 ²¹ G. Dagvadorj, J. M. Fellows, S. Matyjaskiewicz, F. M. Marchetti, I. Carusotto, M. H. Szymanska,
276 Nonequilibrium phase transition in a two-dimensional driven open quantum system. *Phys. Rev. X* **5**,
277 041028 (2015).
- 278 ²² S. Utsunomiya, L. Tian, G. Roumpos, C. W. Lai, N. Kumada, T. Fujisawa, M. Kuwata-Gonokami, A.
279 Löffler, S. Höfling, A. Forchel, Y. Yamamoto, Observation of Bogoliubov excitations in exciton-polariton
280 condensates. *Nature Phys.* **4**, 700 (2008).
- 281 ²³ V. Kohnle, Y. Léger, M. Wouters, M. Richard, M. T. Portella-Oberli, B. Deveaud-Plédran, From single
282 particle to superfluid excitations in a dissipative polariton gas. *Phys. Rev. Lett.* **106**, 255302 (2011).
- 283 ²⁴ V. Kohnle, Y. Léger, M. Wouters, M. Richard, M. T. Portella-Oberli, B. Deveaud, Four-wave mixing
284 excitations in a dissipative polariton quantum fluid. *Phys. Rev. B* **86**, 064508 (2012).
- 285 ²⁵ G. Roumpos, M. Lohse, W. H. Nitsche, J. Keeling, M. H. Szymanska, P. B. Littlewood, A. Löffler, S.
286 Höfling, L. Worschech, A. Forchel, Y. Yamamoto, Power-law decay of the spatial correlation function in

- exciton-polariton condensates. PNAS **109**, 6467–6472 (2012).
- ²⁶ D. N. Krizhanovskii, D. Sanvitto, A. P. D. Love, M. S. Skolnick, D. M. Whittaker, J. S. Roberts, Dominant effect of polariton-polariton interactions on the coherence of the microcavity optical parametric oscillator. Phys. Rev. Lett. **97**, 097402 (2006).
- ²⁷ A. P. D. Love, D. N. Krizhanovskii, D. M. Whittaker, R. Bouchekioua, D. Sanvitto, S. A. Rizeiqi, R. Bradley, M. S. Skolnick, P. R. Eastham, R. Andre, L. S. Dang, Intrinsic decoherence mechanisms in the microcavity polariton condensate. Phys. Rev. Lett. **101**, 067404 (2008).
- ²⁸ S. Kim, B. Zhang, Z. Wang, J. Fischer, S. Brodbeck, M. Kamp, C. Schneider, S. Höfling, H. Deng, Coherent polariton laser. Phys. Rev. X **6**, 011026 (2016).
- ²⁹ S. Dihel, A. Micheli, A. Kantian, B. Kraus, H. Buchler, P. Zoller, Quantum states and phases in driven open quantum systems with cold atoms. Nat. Phys. **4**, 878 (2008).
- ³⁰ J. Keeling, M. H. Szymańska, P. B. Littlewood. Keldysh Green's function approach to coherence in a non-equilibrium steady state: connecting Bose–Einstein condensation and lasing, 293–329 (Springer Berlin Heidelberg, Berlin, Heidelberg, 2010).
- ³¹ P. Kirton, J. Keeling, Nonequilibrium model of photon condensation. Phys. Rev. Lett. **111**, 100404 (2013).
- ³² H. Deng, G. Weihs, D. Snoke, J. Bloch, Y. Yamamoto, Polariton lasing vs. photon lasing in a semiconductor microcavity. PNAS **100**, 15318 (2003).
- ³³ L. V. Butov, Solid-state physics: A polariton laser. Nature **447**, 540–541 (2007).
- ³⁴ J. Klaers, J. Schmitt, F. Vewinger, M. Weitz, Bose–Einstein condensation of photons in an optical microcavity. Nature **468**, 545 (2010).
- ³⁵ M.D. Fraser, S. Hofling, Y. Yamamoto, Physics and applications of exciton-polariton lasers. Nat Mater **15**, 1049 (2016).
- ³⁶ Y. Sun, P. Wen, Y. Yoon, G. Liu, M. Steger, L. Pfeiffer, K. West, D. Snoke, K. Nelson, Bose–Einstein condensation of long-lifetime polaritons in thermal equilibrium. arXiv:1601.02581 (2016).
- ³⁷ A. Chiocchetta, I. Carusotto, Non-equilibrium quasi-condensates in reduced dimensions. EPL (Europhysics Letters) **102**, 67007 (2013).
- ³⁸ J. Keeling, L. Sieberer, E. Altman, L. Chen, S. Diehl, J. Toner, Superfluidity and phase correlations of driven dissipative condensates. Chapter in: Universal Themes of Bose-Einstein Condensation, N.P. Proukakis, D.W. Snoke and P.B. Littlewood (Eds.) (Cambridge University Press, 2017).
- ³⁹ D. N. Krizhanovskii, K. G. Lagoudakis, M. Wouters, B. Pietka, R. A. Bradley, K. Guda, D. M. Whittaker, M. S. Skolnick, B. Deveaud-Pledran, M. Richard, R. Andre, L. S. Dang, Coexisting nonequilibrium condensates with long-range spatial coherence in semiconductor microcavities. Phys. Rev. B **80**, 045317 (2009).
- ⁴⁰ D. Sanvitto, D. N. Krizhanovskii, D. M. Whittaker, S. Ceccarelli, M. S. Skolnick, J. S. Roberts, Spatial structure and stability of the macroscopically occupied polariton state in the microcavity optical parametric oscillator. Phys. Rev. B **73**, 241308(R) (2006).

- 324 ⁴¹ H. Deng, G. S. Solomon, R. Hey, K. H. Ploog, Y. Yamamoto, Spatial coherence of a polariton condensate.
325 Phys. Rev. Lett. **99**, 126403 (2007).
- 326 ⁴² W. H. Nitsche, N. Y. Kim, G. Roumpos, C. Schneider, M. Kamp, S. Höfling, A. Forchel, Y. Yamamoto,
327 Algebraic order and the Berezinskii–Kosterlitz–Thouless transition in an exciton-polariton gas. Phys.
328 Rev. B **90**, 205430 (2014).
- 329 ⁴³ Z. Hadzibabic, P. Kruger, M. Cheneau, B. Battelier, J. Dalibard, Berezinskii–Kosterlitz–Thouless
330 crossover in a trapped atomic gas. Nature **441**, 1118–1121 (2006).
- 331 ⁴⁴ D. Bajoni, E. Semenova, A. Lemaitre, S. Bouchoule, E. Wertz, P. Senellart, J. Bloch, Polariton light-
332 emitting diode in a GaAs-based microcavity. Phys. Rev. B **77**, 113303 (2008).
- 333 ⁴⁵ G. Tosi, G. Christmann, N. G. Berloff, P. Tsotsis, T. Gao, Z. Hatzopoulos, P. G. Savvidis, J. J. Baumberg,
334 Sculpting oscillators with light within a nonlinear quantum fluid. Nat. Phys. **8**, 190 (2012).
- 335 ⁴⁶ E. Wertz, L. Ferrier, D. D. Solnyshkov, R. Johne, D. Sanvitto, A. Lemaître, I. Sagnes, R. Grousson, A. V.
336 Kavokin, P. Senellart, G. Malpuech, J. Bloch, Spontaneous formation and optical manipulation of extended
337 polariton condensates. Nat. Phys. **6**, 860 (2010).
- 338 ⁴⁷ D. Ballarini, D. Caputo, C. Muñoz, M. De Giorgi, L. Dominici, M. Szymańska, W. K., L. Pfeiffer, G.
339 G., F. Laussy, D. Sanvitto, Formation of a macroscopically extended polariton condensate without an
340 exciton reservoir. Phys. Rev. Lett. **118**, 215301 (2017).
- 341 ⁴⁸ L. M. Sieberer, M. Buchhold, S. Diehl, Rep. Prog. Phys. **79**, 096001 (2016).
- 342 ⁴⁹ R. Butté, G. Delalleau, A. I. Tartakovskii, M. S. Skolnick, V. N. Astratov, J. J. Baumberg, G. Malpuech,
343 A. Di Carlo, A. V. Kavokin, J. S. Roberts, Transition from strong to weak coupling and the onset of
344 lasing in semiconductor microcavities. Phys. Rev. B **65**, 205310 (2002).

Acknowledgements

345
346 This work has been funded by the MIUR project Beyond Nano and the ERC project POLAFLOW
347 (Grant N. 308136). M. H. S. acknowledges support from EPSRC (Grants No. EP/I028900/2 and
348 No. EP/K003623/2).

Author contributions

349
350 D.C. and D.B. took and analysed the data. G.D. and M.H.S. performed stochastic numerical
351 simulations. C.S.M. and F.P.L. discussed the results. D.C., D.B., C.S.M., M.D.G., L.D., G.G.,
352 F.P.L. M.H.S. and D.S. co-wrote the manuscript. K.W. and L.N.P. fabricated the sample. D.S.
353 coordinated and supervised all the work.